

ROBUST CONTROL AND PATH PLANNING ALGORITHMS FOR SMALL SATELLITE FORMATION FLYING MISSIONS

Chakravarthini M. Saaj

Space Robotics, Surrey Space Center, University of Surrey, Guildford, Surrey, GU2 7XH, UK
Email: c.saaj@surrey.ac.uk

Saptarshi Bandyopadhyay

Department of Aerospace Engineering, Indian Institute of Technology Bombay, Mumbai 400076, India.
Email: saptarshi_b@iitb.ac.in,

Bijnan Bandyopadhyay

Interdisciplinary Programme in Systems and Control Engineering, Indian Institute of Technology Bombay, Mumbai 400076, India. Email: bijnan@ee.iitb.ac.in

ABSTRACT

Recent advances in small, low cost satellite technology has generated a renewed interest in formation flying missions. One challenging aspect of satellite formation flying missions is collision free navigation and control. In this paper, novel robust control algorithm using Sliding Mode Control is presented for a three-dimensional, high Earth orbit satellite formation scenario. The paper presents the comparison of results of three types of Sliding Mode Controllers (SMC): the first one is a tan-hyperbolic SMC, the second one is a constant plus proportional rate SMC and the third one is a power rate SMC. Hybrid propulsion system minimises the use of on-board power for close formations. Artificial Potential Field method is used for collision-free path planning of the satellites in the formation. Simulation results show that for the formation flying scenario considered in this study, the constant plus proportional rate SMC and the power rate SMC gives better performance over the tan-hyperbolic SMC. Simulation results prove that for the tetrahedron formation considered in this study, the total control effort is less when the constant plus proportional rate controller and the power rate controller are used compared to the tan-hyperbolic sliding mode controller. Very little formation center movement is observed for the three SMCs.

FULLTEXT

I. INTRODUCTION

Small satellites are highly suitable for formation flying missions, where multiple satellites operate together in a cluster or predefined geometry to accomplish the task of a single, conventional large satellite. In comparison to traditional large and expensive satellites, small satellites offer low development cost as it enables use and reuse of commercial off the shelf components in less time. Moreover modular nature of these systems helps in their replacement or up-gradation [1]. However, collision free navigation and control of these satellites is a challenging problem. Moreover, the space debris also poses threats to these small satellites.

On the other hand, it has been observed for a long time that certain living beings tend to perform swarming behavior. Examples of swarms include flocks of birds, schools of fish, herds of animals, and colonies of bacteria. It is known that such a cooperative behavior has certain advantages such as avoiding predators and increasing the chance of finding food but it requires communications and

coordinated decision making. Operational principles from such systems can be used in engineering for developing distributed cooperative control, coordination, and learning strategies for autonomous agent systems such as autonomous multirobot applications, unmanned undersea, land, or air vehicles. The general understanding among biologist is that the swarming behavior is a result of interplay between a long range attraction and short range repulsion between the individuals. A simple model is suggested in [2] composed of a constant attraction term and a repulsion term which is inversely proportional to the square of the distance between two members. In [3] and [4], the biologists have studied the affect on cohesion of a family of attraction/repulsion functions and provide good background and review of the swarm modelling concepts. A similar study on stable swarm aggregations using attraction/repulsion functions from an engineering perspective is done in [5].

Autonomous collision-free reconfiguration is a challenging task and needs to be accomplished with minimal use of on-board power. The propulsion system is one of the key subsystems that determine

the cost and lifetime of the mission. Spacecraft propulsion utilising naturally available electrostatic forces is an emerging technology [6], [7] and spacecrafts could have extremely long lifetimes. Since all forces are internal and so the Coulomb forces cannot alter the total inertial linear and rotational momentum [8], [9]. But the concept has not yet been fully proven to be suitable for a realistic mission. Advancement in this field would be a major breakthrough in propulsion technology. This motivates us to use electrostatic propulsion in combination with electric propulsion for small satellite formation flying missions.

The major focus of this study is on improving the control algorithm using a robust control algorithm using sliding mode control. Intelligent path planning algorithm is designed using Artificial Potential Field (APF) method [10], which is widely used for collision avoidance of mobile robots. This paper presents how satellites in the formation can aggregate towards a goal position, similar to biological swarms and then takes up positions to form a predefined formation. Based on the knowledge of current position, the APF method will optimise the trajectory to generate the next desired formation which will be achieved using the sliding mode controller. Since sliding mode control guarantees robust performance, the impact of external perturbations like solar wind and internal perturbations like change in mass due to fuel consumption will have negligible impact on the performance of the satellite. A comparative study in [11] shows that the tan-hyperbolic SMC gives better performance than the PD controller. As a follow-on study, this paper gives a comparison within the different kinds of sliding mode controllers; namely the tan-hyperbolic SMC, constant plus proportional rate SMC and the power rate SMC. It is envisaged that the results presented in this paper would enable to advance the current small satellite formation flying technology, in addition to enhancing controller performance for a realistic mission scenario.

II. BACKGROUND RESULTS

A. Path Planning Using Artificial Potential Field

Let the formation consists of N individual agents in the n dimensional Euclidean space [12]. The position of the i^{th} agent is described by $\mathbf{x}_i \in \mathbf{R}^n$. It is assumed that there is no time delay and synchronous motion exists. The motion of each agent in the formation is governed by the equation:

$$\dot{\mathbf{x}}_i = \sum_{j=1, j \neq i}^N \mathbf{g}(\mathbf{x}_i - \mathbf{x}_j), \quad i = 1, \dots, N, \quad (1)$$

where $\mathbf{g}(\cdot)$ is an odd function which represents the sum of the function of attraction and repulsion

between the agents. The function $\mathbf{g}(\cdot)$ can be represented by $\mathbf{g}(\mathbf{y}) = -\mathbf{y}[g_a(\|\mathbf{y}\|) - g_r(\|\mathbf{y}\|)]$ where $\mathbf{y} \in \mathbf{R}^n$ is arbitrary and $\|\mathbf{y}\| = \sqrt{\mathbf{y}^T \mathbf{y}}$ is the Euclidean norm [12]. Hence the magnitude and direction of motion of each member is determined as a sum of the attraction and repulsion of all the other members on this member. It is needed for avoiding collisions that the repulsion term $g_r(\|\mathbf{y}\|)$ dominates on short distances and for aggregation that the attraction term $g_a(\|\mathbf{y}\|)$ dominates on large distances. There is a distance δ at which the attraction and the repulsion balance and $g_a(\delta) = g_r(\delta)$. The attraction/repulsion function that we consider in this paper is

$$\mathbf{g}(\mathbf{y}) = -\mathbf{y} \left(a - b \exp\left(-\frac{\|\mathbf{y}\|^2}{c}\right) \right) \quad (2)$$

where a , b and c are positive constants such that $b > a$. Note that the function $\mathbf{g}(\mathbf{y})$ constitutes an artificial potential function, that governs the inter-individual interactions [13]. The term $b \exp(-\|\mathbf{y}\|^2/c)$ represents the repulsion, whereas the term a represents the attraction. This function is repulsive (i.e., $b \exp(-\|\mathbf{y}\|^2/c)$ dominates) for small distances and attractive (i.e., a dominates) for large distances, which is consistent with interindividual attraction/repulsion in biological swarms [4], [14]. Therefore, it constitutes a crude approximation of biological interactions and also allows us to perform stability analysis. The main drawbacks with $\mathbf{g}(\cdot)$ are that it is strongly repulsive but not unbounded for infinitesimally small arguments, which may be needed to avoid collisions, and it has an infinite range, which is inconsistent with biology since no creature has infinite sensing range [12]. By equating $\mathbf{y}(a - b \exp(-\|\mathbf{y}\|^2/c)) = 0$, one can easily find that $\mathbf{g}(\mathbf{y})$ switches sign at the set of points defined as $\mathbf{Y} = \{\mathbf{y} = 0 \text{ or } \|\mathbf{y}\| = \delta = \sqrt{c \ln(b/a)}\}$. The distance δ is the distance at which the attraction and repulsion balance. It is known that there exists such a distance in biological swarms [14], [3].

Equation (1) can be represented also by:

$$\dot{\mathbf{x}}_i = -\nabla_{\mathbf{x}_i} \mathbf{J}(\mathbf{x}), \quad i = 1, \dots, N, \quad (3)$$

where $\mathbf{x}^T = [\mathbf{x}_1^T \dots \mathbf{x}_N^T]$ is the lumped vector of the positions of all the agents and $\mathbf{J}: \mathbf{R}^{nN} \rightarrow \mathbf{R}$ is a potential function [11]. Such potential functions are being used for swarm aggregations, formation control, and multiagent coordination and control under different names. $\mathbf{J}(\mathbf{x})$ and $\mathbf{g}(\mathbf{x})$ are related by equation (1) and (3). The potential $\mathbf{J}(\mathbf{x})$ may represent only the interindividual interactions, or may include also environmental effects, or may be defined for some other purpose. For simplicity, we consider the case in which it does not include any environmental terms. In particular, consider the potential functions of the form

$$\mathbf{J}(\mathbf{x}) = \sum_{i=1}^{N-1} \sum_{j=i+1}^N \mathbf{J}_{ij}(\|\mathbf{x}_i - \mathbf{x}_j\|) \quad (4)$$

where $\mathbf{J}_{ij}(\|\mathbf{x}_i - \mathbf{x}_j\|)$ is the potential between i and j , and can be different for different pairs. Moreover, we assume that $\mathbf{J}_{ij}(\|\mathbf{x}_i - \mathbf{x}_j\|)$ satisfies the following [12].

(A) The potentials $\mathbf{J}_{ij}(\|\mathbf{x}_i - \mathbf{x}_j\|)$ are symmetric and satisfy

$$\nabla_{\mathbf{x}_i} \mathbf{J}_{ij}(\|\mathbf{x}_i - \mathbf{x}_j\|) = -\nabla_{\mathbf{x}_j} \mathbf{J}_{ij}(\|\mathbf{x}_i - \mathbf{x}_j\|) \quad (5)$$

(B) There exists a corresponding function $g_{ar}^{ij}: \mathbf{R}^+ \rightarrow \mathbf{R}^+$ such that

$$\nabla_{\mathbf{y}} \mathbf{J}_{ij}(\|\mathbf{y}\|) = \mathbf{y} g_{ar}^{ij}(\|\mathbf{y}\|) \quad (6)$$

(C) There exist unique distances δ_{ij} , at which we have $g_{ar}^{ij}(\delta_{ij}) = 0$ and $g_{ar}^{ij}(\|\mathbf{y}\|) > 0$ for $\|\mathbf{y}\| > \delta_{ij}$, and $g_{ar}^{ij}(\|\mathbf{y}\|) < 0$ for $\|\mathbf{y}\| < \delta_{ij}$.

Potential functions satisfying these are odd functions, which are attractive on distances $\|\mathbf{y}\| > \delta_{ij}$ and repulsive on distances $\|\mathbf{y}\| < \delta_{ij}$. The distance δ_{ij} is the equilibrium distance at which the attraction and the repulsion balance. It can be shown that the functions satisfying these conditions result in aggregating swarm behavior [13], [5].

One shortcoming of the motion dynamics in equation (4), and therefore, any results related to it, is that it does not correspond to the dynamics of realistic agents [12]. Therefore, the model is, in a sense, a kinematic model for swarm aggregation, formation control, or agent-coordination dynamics. For this reason, the results derived for it serve as proof of concept for the behaviour considered. However, they do not specify how that desired proven behavior could be achieved in engineering applications with given (i.e., predefined) agent (vehicle) dynamics. Nevertheless, they are still of practical interest, and can serve as guidelines for designing swarming engineering multiagent systems. In the next section, we will show how by using the sliding-mode control technique, we can achieve the above type of motion for agents with general fully actuated vehicle dynamics, even in the presence of disturbances and uncertainties.

B. Coulomb Spacecraft Charging

Let us assume that for a swarm of N satellites in GEO, the charge products can be perfectly implemented into individual real satellite charges. For the i^{th} satellite, consider all possible pairs of charge products due to the remaining $N-1$ satellites as $Q_{ij} = q_i q_j, j = 1, \dots, N, i \neq j$. Then the commanded force acting on the i^{th} satellites is [11]:

$$\mathbf{u}_i^c = \sum_{j=1, i \neq j}^N (k_c Q_{ij} / \mathbf{x}_{ij}^2) \exp(-\mathbf{x}_{ij} / \lambda_d) \quad (7)$$

where $k_c = (4\pi\epsilon_0)^{-1} = 8.99 \times 10^9 \text{ Nm}^2/\text{C}^2$ is a constant of proportionality that depends on the permittivity of free space, $\mathbf{x}_{ij} = \|\mathbf{x}_i - \mathbf{x}_j\|$ is the satellite separation and λ_d is the Debye length. The commanded force is calculated using an appropriate control law. Coulomb thrusting makes use of a renewable source of electrical energy and is essentially free from contaminations due to its extremely high fuel efficiency. It is estimated that Coulomb forces of the order of 10-1000 micro-Newtons, comparable to the thrust developed by conventional electric propulsion, can be produced on short timescales, using less than 1 Watt of on board power [15], [16]. A navigation strategy cannot be implemented with a purely Coulomb-based control concept, as sufficient thrust cannot be produced when separation between individual satellites is large. General charge control strategies to control the relative motion of N satellites are still an active area of research. At this stage this analysis is still idealized and will be refined for particular charge implementation strategies in the future.

C. Comparison of Proportional-Derivative (PD) Controller with tan-hyperbolic Sliding Mode Controller

Consider the general non-linear inertial equation of motion of the swarm agent represented by [11]

$$\mathbf{M}_i(\mathbf{x}_i) \ddot{\mathbf{x}}_i + \mathbf{f}_i(\mathbf{x}_i, \dot{\mathbf{x}}_i) = \mathbf{u}_i^a, \quad 1 \leq i \leq N \quad (8)$$

where, $\mathbf{x}_i \in \mathbf{R}^n$ is the position vector of agent i , $\mathbf{M}_i \in \mathbf{R}^{n \times n}$ is the mass or inertia matrix and is assumed to be non-singular, $\mathbf{f}_i(\mathbf{x}_i, \dot{\mathbf{x}}_i) \in \mathbf{R}^n$, N is the number of agents in the swarm, $\mathbf{u}_i^a \in \mathbf{R}^n$ is the control input delivered by the actuators. The additive term $\mathbf{f}_i(\mathbf{x}_i, \dot{\mathbf{x}}_i)$ is assumed to be of the form

$$\mathbf{f}_i(\mathbf{x}_i, \dot{\mathbf{x}}_i) = \mathbf{f}_i^k(\mathbf{x}_i, \dot{\mathbf{x}}_i) + \mathbf{f}_i^u(\mathbf{x}_i, \dot{\mathbf{x}}_i) \quad (9)$$

where $\mathbf{f}_i^k(\mathbf{x}_i, \dot{\mathbf{x}}_i)$ represents the known part and $\mathbf{f}_i^u(\mathbf{x}_i, \dot{\mathbf{x}}_i)$ is the unknown part of the system dynamics. Here \mathbf{u}_i^a denote the actual force available from the hybrid thrusters to i^{th} satellite for changing its manoeuvre. In the APF method, corresponding to equation (8), the motion of the individual agent is governed by equation (3).

The PD controller for the i^{th} satellite can be expressed in terms of the position and velocity errors as [11]:

$$\begin{aligned} \mathbf{u}_i^c = & \mathbf{f}_i^k(\mathbf{x}_i, \dot{\mathbf{x}}_i) + \mathbf{M}_i^o \ddot{\mathbf{x}}_i^r - K_{vi}(\dot{\mathbf{x}}_i^r - \dot{\mathbf{x}}_i) \\ & - K_{pi}(\mathbf{x}_i^r - \mathbf{x}_i), \\ & 1 \leq i \leq N \end{aligned} \quad (10)$$

where, \mathbf{x}_i^r is the desired position, \mathbf{x}_i is the actual position of i^{th} satellite respectively. \mathbf{M}_i^o is the nominal (known) mass of the satellite. The parameters K_{p_i} and K_{v_i} are the proportional and the derivative gains, respectively. Here \mathbf{u}_i^c denote the force requested by the controller, from the hybrid thrusters to i^{th} satellite, for changing its manoeuvre. Note that this controller requires the second derivative with respect to time of the desired (reference) trajectory $\ddot{\mathbf{x}}_i^r$ which is not needed by the sliding mode controller.

For the sliding mode control method, the n dimensional sliding manifold for i^{th} satellite is chosen as [11]:

$$\mathbf{s}_i = \dot{\mathbf{x}}_i + \nabla_{\mathbf{x}_i} \mathbf{J}(\mathbf{x}) = 0, \quad i = 1, \dots, N, \quad (11)$$

Note that here the potential function $\mathbf{J}(\mathbf{x})$ is not static. It depends on the relative positions of the individuals in the swarm and need to satisfy certain assumptions made in [12]. Once all the satellite reach the respective sliding manifolds $\mathbf{s}_i = 0$, equation (11) reduces to $\dot{\mathbf{x}}_i = -\nabla_{\mathbf{x}_i} \mathbf{J}(\mathbf{x})$ which is same as the motion (3) of the satellite swarm. A sufficient condition for sliding mode to occur given in [17] is satisfaction of:

$$\mathbf{s}_i^T \dot{\mathbf{s}}_i < 0, \quad i = 1, \dots, N \quad (12)$$

This does not guarantee that starting from any initial point in the state space; the sliding manifold is reached in finite time. Further, if a stronger condition

$$\mathbf{s}_i^T \dot{\mathbf{s}}_i < -\varepsilon \|\mathbf{s}_i\|, \quad i = 1, \dots, N \quad (13)$$

is satisfied, then it is guaranteed that sliding mode will occur in finite time. In order to achieve this objective, the sliding mode controller is given by:

$$\mathbf{u}_i^c = -\mathbf{u}_i^o \operatorname{sgn}(\mathbf{s}_i) + f_i^k(\mathbf{x}_i, \dot{\mathbf{x}}_i) \quad (14)$$

where, $\operatorname{sign}(\mathbf{s}_i) = [\operatorname{sign}(s_{i_1}) \dots \operatorname{sign}(s_{i_N})]^T$. The gain of the control input is chosen as $\mathbf{u}_i^o > (1/\mathbf{M}_{i_l})(\mathbf{M}_{i_u} f_i + \mathbf{J} + \varepsilon_i)$, for some $\varepsilon_i > 0$, and equation (13) is guaranteed. Here \mathbf{M}_{i_l} and \mathbf{M}_{i_u} are the known lower and upper bounds of the inertia matrix respectively.

In the above controller, only the known part $f_i^k(\mathbf{x}_i, \dot{\mathbf{x}}_i)$ of the disturbance is considered. For practical implementations, a major inherent drawback of sliding mode controllers is the chattering phenomenon. Finite high frequency oscillations are generated due to the presence of unmodelled fast dynamics of the sensors and actuators and due to non-ideal realization of the relay characteristics of the SMC. In order to reduce the chattering phenomenon, the $\operatorname{sgn}(\mathbf{s}_i)$ term in the controller equation (14) can be replaced by a smooth approximation using $\tanh(\beta \mathbf{s}_i)$. Note that the chattering may be eliminated by this smoothing function but the controller will not be robust against

uncertainties. It only ensures that the resulting sliding motion will lie in a close vicinity of the sliding manifold. The sliding mode controller used is:

$$\mathbf{u}_i^c = -\mathbf{u}_i^o(x) \tanh(\beta \mathbf{s}_i) + f_i^k(\mathbf{x}_i, \dot{\mathbf{x}}_i) \quad (15)$$

Since the dynamics of the hybrid propulsion actuator are not considered during the design of the controllers, the control variable \mathbf{u}_i^c in equation (10) for PD controller and in equation (15) for the sliding mode controller, is used as the control input \mathbf{u}_i^a in equation (8). The simulation results in [11] show that, for the scenarios considered in that study, the control effort required by the individual satellite is far less with sliding mode controller when compared to that using PD controller. It is observed that the swarm center movement is less with sliding mode control facilitating quicker achievement of the formation and hence greater fuel saving. Moreover, sliding mode controller is inherently insensitive to parameter variations and disturbances once in the sliding mode, thereby eliminating the necessity of exact spacecraft modeling. In this paper, a different kind of sliding mode control algorithm has been used for swarm formation. This algorithm is based on the constant plus proportional rate reaching law and power rate reaching law, along with a sat function within the boundary layer.

III. SMC BASED ON BOUNDARY LAYER TECHNIQUE

A. *Sliding Mode Controller using Constant plus Proportional Rate Reaching Law*

The constant plus proportional reaching law with the replacement of the sgn function by the sat function is given as [18]:

$$\dot{\mathbf{s}}_i = -q \mathbf{s}_i - \varepsilon \operatorname{sat}\left(\frac{\mathbf{s}_i}{\phi_i}\right) \quad (16)$$

Here, when the trajectory enters into a small vicinity of the sliding surface (denoted by Φ), the control does not switch and hence chattering is eliminated. Differentiating equation (11) with respect to time gives

$$\dot{\mathbf{s}}_i = \ddot{\mathbf{x}}_i + \frac{d}{dt} \nabla_{\mathbf{x}_i} \mathbf{J}(\mathbf{x}), \quad i = 1, \dots, N, \quad (17)$$

Equating equation (16) and (17) gives

$$\ddot{\mathbf{x}}_i + \frac{d}{dt} \nabla_{\mathbf{x}_i} \mathbf{J}(\mathbf{x}) = -q \mathbf{s}_i - \varepsilon \operatorname{sat}\left(\frac{\mathbf{s}_i}{\phi_i}\right) \quad (18)$$

Substituting equation (18) in the general non-linear inertial equation of motion of the swarm agent (8) gives the control input

$$\mathbf{u}_i = f_i(\mathbf{x}_i, \dot{\mathbf{x}}_i) - \mathbf{M}_i q \mathbf{s}_i - \mathbf{M}_i \varepsilon \text{sat}\left(\frac{\mathbf{s}_i}{\phi_i}\right) - \mathbf{M}_i \frac{d}{dt} \nabla_{\mathbf{x}_i} \mathbf{J}(\mathbf{x}) \quad (19)$$

When this control input is applied and all the satellite reach the respective sliding manifolds $\mathbf{s}_i = 0$, the dynamics of the system reduces to $\dot{\mathbf{x}}_i = -\nabla_{\mathbf{x}_i} \mathbf{J}(\mathbf{x})$ which is same as the motion (3) of the satellite swarm.

B. Sliding Mode Controller using Power Rate Reaching Law

The power rate reaching law with sat function is given as [18]:

$$\dot{\mathbf{s}}_i = -k |\mathbf{s}_i|^\alpha \text{sat}\left(\frac{\mathbf{s}_i}{\phi_i}\right) \quad (20)$$

Equating equation (17) and (20) gives

$$\ddot{\mathbf{x}}_i + \frac{d}{dt} \nabla_{\mathbf{x}_i} \mathbf{J}(\mathbf{x}) = -k |\mathbf{s}_i|^\alpha \text{sat}\left(\frac{\mathbf{s}_i}{\phi_i}\right) \quad (21)$$

Substituting equation (21) in the general non-linear inertial equation of motion of the swarm agent (8) gives the control input

$$\mathbf{u}_i = f_i(\mathbf{x}_i, \dot{\mathbf{x}}_i) - \mathbf{M}_i k |\mathbf{s}_i|^\alpha \text{sat}\left(\frac{\mathbf{s}_i}{\phi_i}\right) - \mathbf{M}_i \frac{d}{dt} \nabla_{\mathbf{x}_i} \mathbf{J}(\mathbf{x}) \quad (22)$$

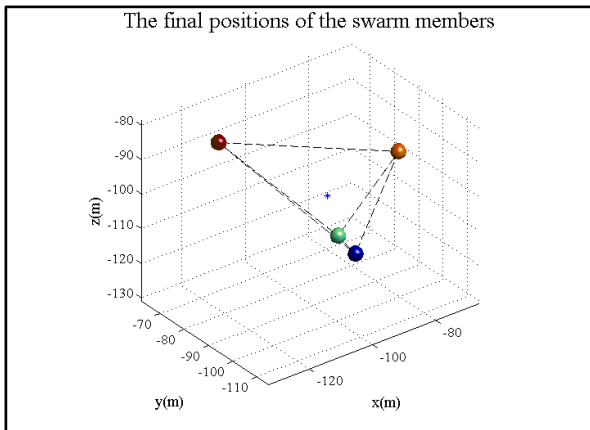
When this control input is applied and all the satellite reach the respective sliding manifolds $\mathbf{s}_i = 0$, the dynamics of the system reduces to $\dot{\mathbf{x}}_i = -\nabla_{\mathbf{x}_i} \mathbf{J}(\mathbf{x})$ which is same as the motion (3) of the satellite swarm.

IV. SIMULATION RESULTS

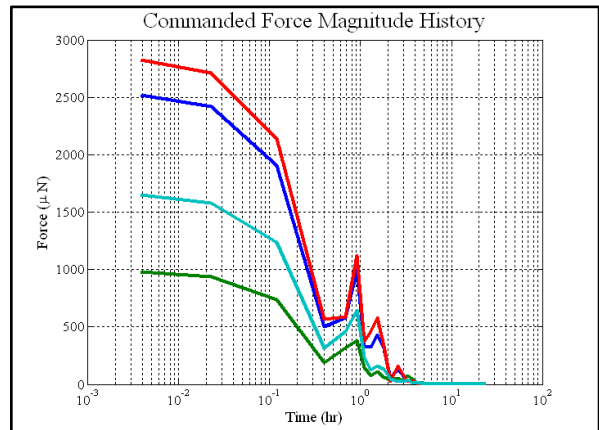
The goal of this section is to simulate a tetrahedron formation using APF method, Coulomb

forces and compare the three sliding mode controllers. The inter-satellite separation is to be maintained at 50 meter. The parameter a in equation (2) is computed in order to achieve the balance of attraction and repulsion between any two satellites at the desired distance d in the final tetrahedron formation. Let $b = 5 * 10^{-5}$, $c = 100$, $d = 50$ and $a = b \exp(-d^2/c)$. For formation control, each agent in the formation is pre-assigned a desired relative position in the final formation. The satellites are propelled using the electrostatic propulsion, in combination with conventional electric thrusters as hybrid propulsion system minimises the use of on-board power for close formations. The actuator dynamics, the environmental perturbations and other factors except the controllers are the same as described in [11]. This paper deals with the comparison of the three sliding mode controllers. It is assumed that both the uncertainty in the satellite mass and external perturbation is same for all the controller designs. The bounds of the uncertainty in mass are set as $\pm 50\%$ of the nominal mass of the satellite. The bound on the known disturbance is set to $2mN$.

The simulation plots for the three Sliding Mode Controllers are shown in Fig. 1. It is assumed that initially the satellites are at rest with an average inter-satellite separation of around 2.7 km. With time, the four satellites move to their required final inter-satellite separation of 50 meter and form the required tetrahedron formation while avoiding collisions. Note that for this particular formation there is no local minima and therefore the local minima problem inherent in the potential functions method is not present here (and the formation can be achieved globally). The simulations were run for 1 day (86400 seconds). The objective in this study is to compare the properties of the three sliding mode controllers and not to test the effectiveness of the potential functions method.



(a)



(b)

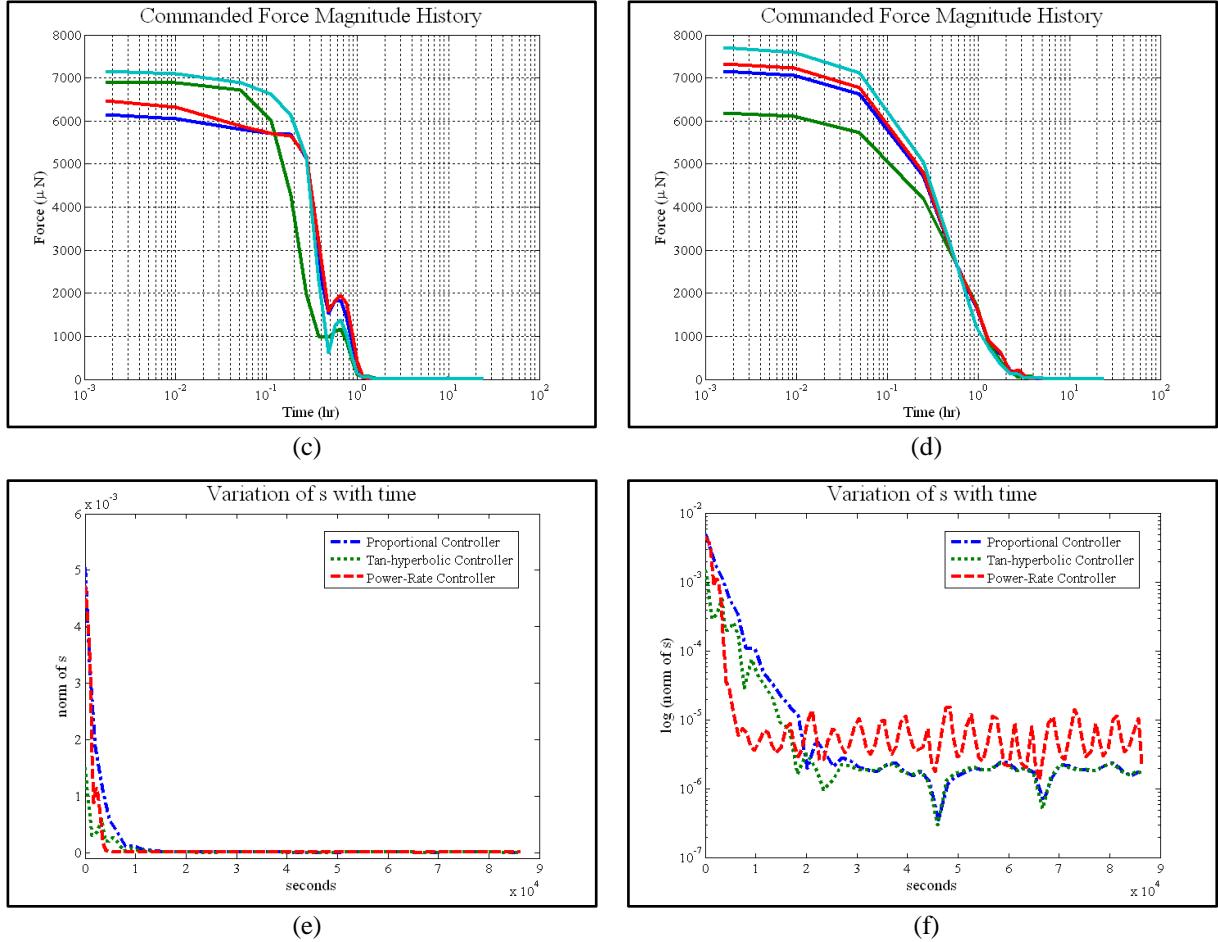


Fig. 1. Simulation results for tetrahedron formation: (a) Final swarm formation; (b), (c) and (d) Commanded Force Magnitude History; (e) and (f) Variation of the norm of s with time for the three SMC

Fig. 1 (a) shows the final formation positions of the satellites and the center of the formation is represented by ‘*’. Very little formation center movement was observed for all the three sliding mode controllers due to the inherent invariance or robustness properties of the method. A large formation center movement was seen for PD controller in [11]. The center movement can lead to delay in achieving the final formation and can change the final orbit of the swarm. The commanded force magnitude history (control inputs) for the tan-hyperbolic SMC, the power rate SMC and the constant plus proportional SMC for all the four satellites are shown in Fig. 1 (b), (c) and (d) respectively. It is observed that the magnitude of the control effort is minimum for the tan-hyperbolic SMC. The duration of the control effort is less for the power rate SMC and least for the constant plus proportional SMC. Hence, if the actuator doesn’t saturate, then the constant plus proportional SMC and power rate SMC will cause the satellites to reach their respective sliding manifolds faster. Fig. 1 (e) and (f) show the variation of the norm of s with time in a linear and logarithmic scale respectively. Norm of s is defined as $\|s\| = \sqrt{(\sum_{i=1}^n s_i^2)/n}$. From the linear plot it is seen that the power-rate SMC is fastest at reaching

the sliding mode manifold, as seen in [18]. From the logarithmic plot it is seen that the norm of s in power rate SMC has an oscillating nature. The offset in the norm of s is due to computational limitations and inaccuracies due to discretization.

V. CONCLUSION

The paper presented a comparative study of three robust control algorithms, based on sliding mode control for satellite formation flying missions. The simulation results prove that the power rate SMC and the constant plus proportional SMC are faster in reaching the sliding mode manifolds for the satellites. This helps in achieving the formation faster. The minimum swarm center movement for all the three SMCs result in lot of savings on onboard fuel. The use of electrostatic propulsion minimises the use of on-board power for tight formation in the high Earth orbits and hence increase the overall lifetime of the mission. The use of APF method guarantees collision free navigation and reduces the computational load, as this approach doesn’t involve extensive map building. The path planning and control algorithms presented in this work can be adapted for low Earth orbit

formation flying missions as well. Simulation results prove that inherent robustness of the sliding mode controllers make this controller suitable for satellite formation flying missions. Further research is under progress to validate the suitability of sliding mode control for realistic formation flying missions.

VI. ACKNOWLEDGEMENTS

The Royal Society, UK, support this work through the International Joint Project, which commenced in April 2009. Saptarshi Bandyopadhyay also received partial travel support from the Indian Institute of Technology, Bombay.

VII. REFERENCES

- [1] A. Das, R. Cobb and M. Stallard, "TechSat 21 - A revolutionary concept in distributed space based sensing," *Proceedings of the Guidance, Navigation and Control Conference*, AIAA-98-5255, Boston, MA, pp. 1-6, 1998.
- [2] C. M. Breder, "Equations descriptive of fish schools and other animal aggregations," *Ecology*, Vol. 35 No. 3, pp. 361-370, 1954.
- [3] K. Warburton, J. Lazarus, "Tendency-distance models of social cohesion in animal groups," *Journal of Theoretical Biology*, Vol. 150, pp. 473-488, 1991.
- [4] A. Okubo, "Dynamical aspects of animal grouping: swarms, schools, flocks, and herds," *Advances in Biophysics*, Vol. 22, pp. 1-94, 1986.
- [5] V. Gazi, Kevin M. Passino, "A class of Attraction/Replulsion Functions for Stable Swarm Aggregations," *International Journal of Control*, Vol. 77 No. 18, pp. 1567-1579, 2004.
- [6] L. B. King, G. G. Parker, S. Deshmukh and J. H. Chong, "Propellantless Control of Spacecraft Swarms using Coulomb Forces," *NIAC Final Report*, 2002.
- [7] H. Schaub, G. G. Parker and L. B. King, "Challenges and Prospects of Coulomb Spacecraft Formations," *AAS John L. Junkins Astrodynamics Symposium*, AAS-03-278, College Station, TX, 2003.
- [8] E. G. Mullen, M. S. Gussenhoven, D. A. Hardy, "SCATHA Survey of High-Voltage Spacecraft Charging in Sunlight," *Journal of the Geophysical Sciences*, Vol. 91, pp. 1074-1090, 1986.
- [9] H. Schaub, M. Kim, "Orbit Element Difference Constraints for Coulomb Satellite Formations," *AIAA/AAS Astrodynamics Specialist Conference*, AIAA 04-5213, Providence, Rhode Island, 2004.
- [10] O. Khatib, "Real-Time Obstacle Avoidance for Manipulator and Mobile Robots," *The International Journal of Robotics Research*, Vol. 5 No. 1, pp. 90-98, 1986.
- [11] C. M. Saaj, V. Lappas, D. Richie, H. Schaub and V. Gazi, "Satellite Formation Flying: Robust Algorithms for Propulsion, Path Planning and Control", *Proceedings European Control Conference*, Budapest, Hungary, 23-26 August 2009.
- [12] V. Gazi, "Swarm Aggregations using Artificial Potentials and Sliding Mode Control," *IEEE Transactions on Robotics*, Vol. 21 No. 6, pp. 1208-1214, 2005.
- [13] V. Gazi, Kevin M. Passino, "Stability Analysis of Swarms," *IEEE Transactions on Automatic Control*, Vol. 48 No. 4, 2003.
- [14] D. Grünbaum, A. Okubo, "Modeling social animal aggregations," *Frontiers in Theoretical Biology*, Springer-Verlag, New York, 1994.
- [15] M. Martinez-Sanchez, J. E. Pollard, "Spacecraft Electric Propulsion - An Overview," *Journal of Propulsion and Power*, Vol. 14 No. 5, pp. 688-699, 1998.
- [16] H. B. Garrett, A. C. Whittlesey, "Spacecraft Charging, An Update," *IEEE Transactions on Plasma Science*, Vol. 28 No. 6, pp. 2017-2028, 2000.
- [17] V. I. Utkin, "Equations of the slipping regime in discontinuous systems: I," *Automation and Remote Control*, Vol. 32, pp. 1897-1907, 1971.
- [18] John Y. Hung, Weiging Gao, James C. Hung, "Variable Structure Control: A Survey," *IEEE Transactions on Industrial Electronics*, Vols. 40, No. 1, February 1993.
- [19] V. Gazi, K. M. Passino, "Stability Analysis of social foraging swarms," *IEEE Transactions on Systems, Man, and Cybernetics - Part B: Cybernetics*, Vol. 34 No. 1, pp. 539-557, February 2004.
- [20] Chakravartini M. Saaj, Vaios Lappas, Dave Richie, Mason Peck, Brett Streetman, Hanspeter Schaub, Dario Izzo, "Electrostatic Forces for Satellite Sawrm Navigation and Reconfiguration," Study ID AO4919 05/4107, 2006.